Icarus 208 (2010) 558–564

Contents lists available at ScienceDirect

Icarus

journal homepage: www.elsevier.com/locate/icarus

Illumination conditions of the south pole of the Moon derived using Kaguya topography

D.B.J. Bussey [a,*], J.A. McGovern [a], P.D. Spudis [b], C.D. Neish [a], H. Noda [c], Y. Ishihara [c], S.-A. Sørensen [d]

[a] The Johns Hopkins University Applied Physics Laboratory, 11100 Johns Hopkins Road, Laurel, MD 20723, USA
[b] Lunar and Planetary Institute, 3600 Bay Area Blvd., Houston, TX 77058, USA
[c] National Astronomical Observatory of Japan, 2-12 Hoshigaoka, Mizusawa, Oshu, Iwate 023-0861, Japan
[d] University College London, Gower Street, London WC1E 6BT, United Kingdom

ARTICLE INFO

Article history:
Received 25 September 2009
Revised 26 February 2010
Accepted 24 March 2010
Available online 24 April 2010

Keywords:
Moon
Moon, Surface
Photometry

ABSTRACT

We have used the Kaguya laser altimeter-derived topography to conduct a comprehensive study of the illumination conditions at the Moon's south pole. We have determined, by comparing simulated and actual Clementine images, that the Kaguya topography can be used to generate realistic illumination conditions. We generated an average illumination map for the year 2020 for the lunar south pole region. From this we identified the areas that receive the most illumination. The place receiving the most illumination (86% of the year) is located close to the rim of Shackleton crater at 88.74°S 124.5°E. However two other areas, less than 10 km apart from each other, are collectively lit for 94% of the year. We found that sites exist near the south pole that are continuously lit for several months during summer. We were also able to map the locations and durations of eclipse periods for these areas. Finally we analyzed the seasonal variations in lighting conditions, from summer to winter, for key areas near the south pole. We conclude that areas exist near the south pole that have illumination conditions that make them ideal candidates as future outpost sites.

1. Introduction

The lunar polar regions experience unusual illumination conditions that make them attractive candidates sites for future exploration, both robotic and human. This is a result of the Moon's spin axis being nearly perpendicular to the ecliptic plane, it is tilted at ~1.5° (Ward, 1975). Portions of the interiors of impact craters near the poles are known to be deep enough to ensure that they never see the Sun. Such regions have been both modeled (Vasavada et al., 1999), and more recently, measured (Paige et al., 2010) to be extremely cold, so cold that they act as cold traps for any volatile molecules that enter them. Several volatile-delivery mechanisms exist with cometary and asteroid impacts likely being the largest provider of volatiles. Conversely, topographically high regions have the possibility of being illuminated for far more than the typical 50% of the time that is experienced in the equatorial regions. The possibility of locations receiving long portions of continuous illumination, in close proximity to areas that may contain water ice (e.g. Nozette et al., 2001) makes the Moon's polar regions potentially ideal future outpost sites.

2. Previous results

2.1. Image analysis

Quantitative illumination maps of both lunar poles have been produced using Clementine images (Bussey et al., 1999, 2005). The south pole map was produced by examining data acquired just after mid-winter in the southern hemisphere to determine how the lighting changed during the lunar day as a function of Sun direction. No areas of constant illumination were found to exist, at the 500 m/pixel scale of the data. However, two regions were discovered (one on the rim of Shackleton, and the other located 15 km away along a ridge), that received illumination >70% of the time and were collectively lit >98% of the time. One flaw with the data were that data gaps existed where no illumination information was available for sub-solar longitude gaps of up to 20°, forcing approximations to be made. An analysis of AMIE data revealed the presence of a hill near the rim of Shackleton that is illuminated for an entire day during lunar summer.

2.2. Simulations

Clementine provided only 71 days of temporal coverage that is inadequate to fully quantify and characterize the polar illumination

* Corresponding author. Address: The Johns Hopkins University Applied Physics Laboratory, 11100 Johns Hopkins Road, Laurel, MD 20723, USA.
E-mail address: ben.bussey@jhuapl.edu (D.B.J. Bussey).

0019-1035/$ - see front matter © 2010 Elsevier Inc. All rights reserved.
doi:10.1016/j.icarus.2010.03.028

conditions. An alternative technique is to use topographic data to simulate surface lighting conditions. This has the benefit of permitting the study of all possible illumination conditions. Margot et al. (1999) produced a Digital Elevation Model (DEM) of the Moon's south-polar region from Earth-based radar measurements and then used it to calculate the amount of permanent shadow in the region. The Margot DEM had a spatial resolution of 150 m and a vertical resolution of 50 m, covering a region within approximately 7° latitude of the nearside of the south pole, with significantly less coverage on the farside. We conducted an initial simulation study using the Margot DEM. We ran several simulations using lighting parameters that matched those of actual images. Comparison of the simulated images with the Clementine images revealed that for sub-solar longitudes corresponding to the nearside, the simulation matched the actual image very well indicating the data covering the nearside to be representative of local lunar topography. However, simulations with farside sub-solar longitudes resulted in predicted illumination conditions that did not match the actual illumination conditions as seen in the Clementine images. This was not surprising given that the DEM can only have limited farside coverage due to the data that is used to generate the DEM being acquired from Earth. Our conclusion was that whilst the radar-derived topography represented the best available polar topography at that time, and was of a high quality its lack of farside coverage prevented it from being used to accurately simulate for all lighting directions and therefore could not be used to conduct the kind of study we propose here (Bussey et al., 2001).

Zuber and Garrick-Bethell (2005) used the Margot et al. (1999) radar-derived DEM to predict the mean annual illumination in the polar regions. However, because the Margot DEM does not produce realistic simulated images for conditions when the sunlight direction is on the far side of the Moon, this model is at least partly incorrect. Zuber and Garrick-Bethell (2005) do not show any comparisons of simulated images with actual images.

A study was conducted using idealized, but realistic, crater shapes (Pike, 1977) to investigate the amount of permanent shadow in simple craters (i.e. bowl-shaped craters less then 20 km in diameter) near the lunar poles (Bussey et al., 2003). They discovered that simple craters over 10° latitude from a pole still contains portions of their interiors that are permanently shadowed. The total amount of permanent shadow inside simple craters is several 1000 km^2.

A more detailed illumination study recently became possible with the partial release of the Kaguya laser-derived topography data set. Kaguya was a lunar orbiter, launched in 2007, which mapped the Moon from a 100 km polar orbit for 2 years. Kaguya (known as SELENE before launch) carried an extensive suite of instruments that conducted a comprehensive study of the lunar surface (Kato et al., 2008). Some of the most visibly stunning results have come from the High Definition (HD) cameras that took several movies (often limb looking) as the spacecraft crossed the poles. In addition to being visually stunning, these have also provided information on polar lighting, as will be described in the section below. The Kaguya mission ended when the spacecraft impacted the lunar surface (near 65.5°S, 80.4°E) in June 2009. We report the results of this new illumination study here.

3. The technique

The primary data set used in this study is a polar Digital Elevation Model (DEM) derived from the laser altimeter experiment. The laser altimeter on Kaguya used a 1064 nm laser firing at 1 Hz (with a corresponding along track spacing of ~1.6 km). Spot size on the lunar surface was 40 m and the vertical accuracy was 5 m (Noda et al., 2008). These data were used to produce a 64 pixels/° (474 m/pixel) spatial resolution DEM covering from 85°S to 90°S.

We have developed software (called LunarShader) that precisely simulates the illumination conditions using a topography data set and precise Sun–Earth–Moon ephemeris data or a user-chosen Sun position. The LunarShader software is initialized with a time in UTC format. With that information the software uses the NAIF/SPICE library and kernels to determine the Earth–Moon–Sun geometry. Once the geometry is specified the software steps through each point in the user specified Digital Elevation Model (DEM) and constructs a list of elevation values along a geodesic from the point in question to the sub-light source point (Sun or Earth), or as close as it can get within the boundaries of the DEM. The list is then analyzed to see if any part of the Sun is blocked by terrain along the geodesic path. If the point is completely blocked a value of zero is assigned to the surface light level, if completely unblocked a value of one is assigned. For cases of partial blockage a sigmoid function is used to determine the illumination level. The process just described only accounts for shadowing. The LunarShader also has the ability to apply a photometric function to produce a realistically lit surface. Other options exist for producing colored slope, color-coded elevation, and relief shading maps.

We have used LunarShader to run multiple lighting simulations using a Kaguya DEM to characterize the illumination conditions in the Moon's south-polar region. Noda et al. (2008) ran similar simulations (using a slightly earlier data set) to deduce the average amount of time that locations were illuminated over the course of a year. Key results of their work were that no places are constantly illuminated, but areas do exist that receive sunlight for >80% of the time. We have used the DEM to characterize the illumination conditions in more detail. Specifically we have addressed four topics:

1. 'Clementine comparison', where we have run LunarShader with illumination conditions identical to those of a Clementine image. We then compare the simulated illumination conditions with those displayed in a real image. We have done this for several images.
2. 'Permanently shadowed regions', we have determined which regions receive no Sun and/or Earth illumination.
3. 'Illumination profiles for key sites', for areas that receive the most illumination we plot out their lighting history over the course of an entire year.
4. 'Seasonal variations', we quantitatively consider the difference in illumination between summer and winter.

All the maps produced in this work cover an area within 4° latitude of the south pole. This is because the available topography covers the 5° closest to the pole as a small amount of topography is required by the software in order to predict precisely the lighting conditions for the region closest to the pole.

4. Results

4.1. Clementine comparison

The Clementine UVVIS image data is the primary data set that has been used to investigate the lunar polar illumination conditions thus far. Clementine orbited the Moon in a 5-h elliptical polar orbit for 71 days in early 1994 (Nozette et al., 1994). The UVVIS instrument, a 384 × 288 CCD camera, acquired data over each pole every other orbit, thus providing a snapshot of the illumination conditions once every 10 h. Data collections began just after mid-winter for the Moon's southern hemisphere. We have used these data to test the accuracy of the Kaguya topography data.

Specifically we ran multiple simulations using the same lighting conditions as actual 750 nm UVVIS images. Some examples of these are shown in Fig. 1. The two examples have almost diametrically opposite sub-solar longitudes, one from a nearside direction and one from a farside direction. The Kaguya topography appears to produce simulations that very closely resemble the actual illumination conditions, including fairly small features.

If the images are co-registered and blinked we find that the simulation is amazingly accurate, predicting even small-scale features. We attempt to show this in Fig. 2 which shows a merged Clementine and simulation product.

We conclude that the Kaguya data is the first topography data of sufficient fidelity and spatial coverage that can be used to predict illumination conditions for all Sun positions without requiring an image to provide ground truth and thus reflects the first time that it has been possible to fully characterize the lunar polar illumination conditions.

4.2. Permanently shadowed regions

Simulations were run to calculate the extent of the permanent shadow in the south pole region. Using JPL's Horizons database we looked at a 1000 years worth of ephemerides data and determined the maximum and minimum sub-solar latitude over that period to be 1.59°. We also checked that the extremes in solar elevation each year occur over all longitudes. We then ran simulations for different solar azimuths but keeping the solar elevation corresponding to the 1000-year high. This allows us to determine which regions remain shadowed over geologic periods of time; the result is shown in Fig. 3. We also calculated the locations of Earth shadow

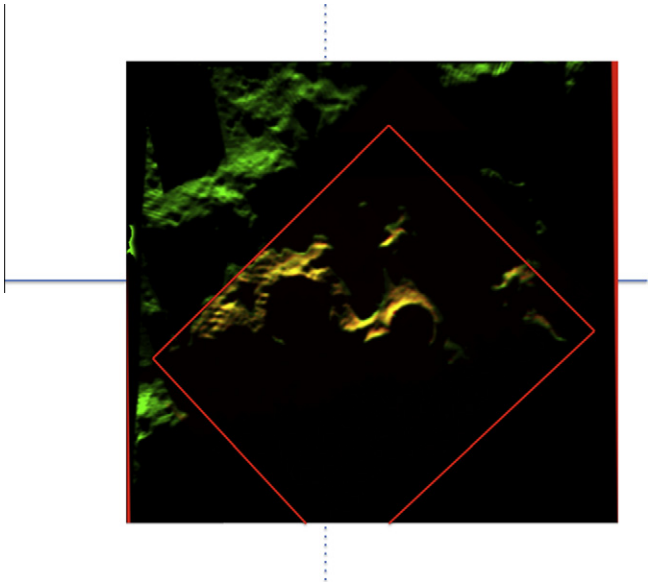

Fig. 2. This was produced be merging Fig. 1A and B. It shows that the simulation using the Kaguya data very accurately predicted the actual illumination conditions.

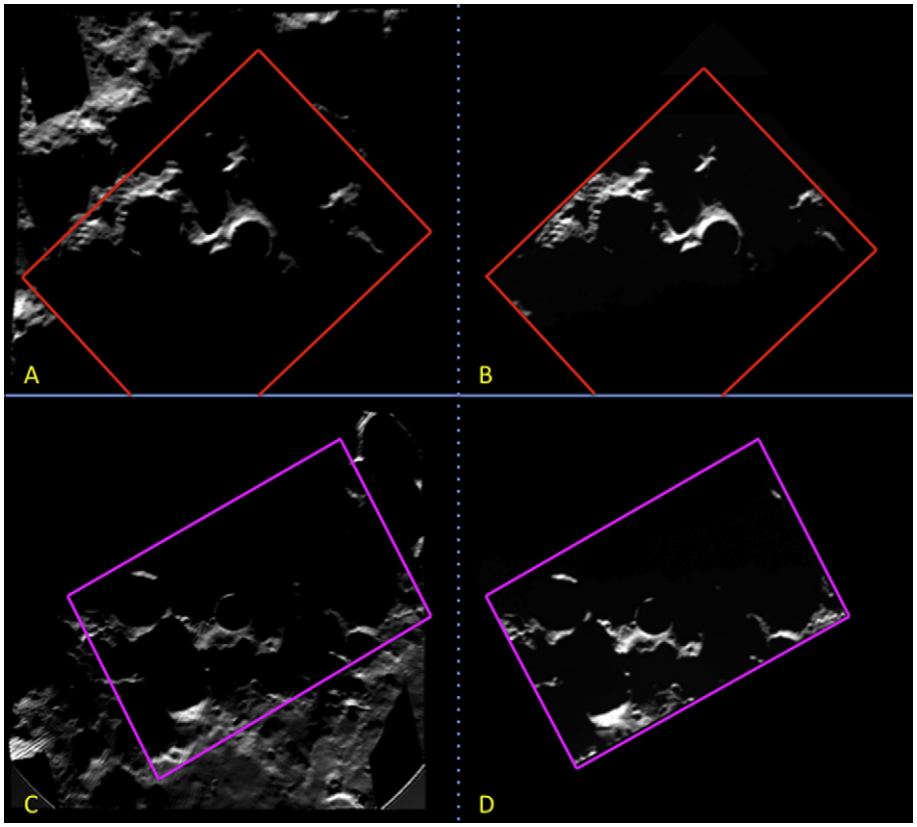

Fig. 1. A comparison between two south-polar Clementine 750 nm UVVIS images and Kaguya-DEM simulations which have the same lighting geometries. In all these images the south pole is located at the center of the image and the 0° longitude line is towards the top of the image. Figure B is Clementine frame lub0040a.317 which has a sub-solar longitude of 15°W. Figure A is the Kaguya simulation. Note that the simulations cover a much larger areal extent than the Clementine images. The red box shows the approximate areal extent of the Clementine image. The black region outside of the red box in B is where there is no data; it does not represent areas that are dark. Figure D is Clementine frame lub0032a.245 which has a sub-solar longitude of 167°E. The simulation shown in Figure C accurately predicts the actual illumination conditions. The areal extent of the Clementine image is shown by the magenta box. (For interpretation of the references to color in this figure legend, the reader is referred to the web version of this article.)

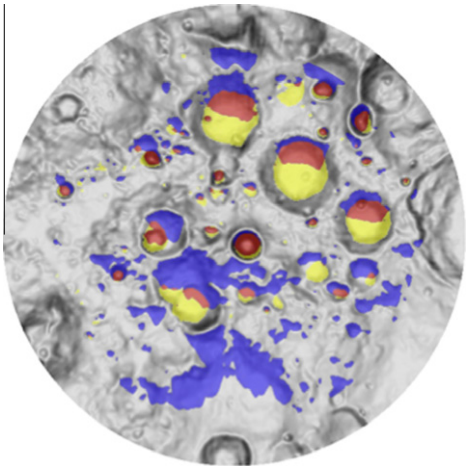

Fig. 3. A map of permanent shadow within 4° of the south pole. Areas shown in red and yellow are permanently shadowed from the Sun. Areas in blue and red are permanently Earth shadowed. Areas in red are also shadowed from both the Sun and the Earth. The map covers from 85°S to the pole, 0° longitude is towards the top of the image. (For interpretation of the references to color in this figure legend, the reader is referred to the web version of this article.)

within 4° of the south pole. We calculate there to be 5058 km^2 of permanent shadow (shown in red and yellow in Fig. 3), 44% of which is also Earth shadowed (shown in red). There is a total of 10,520 km^2 of areas that are always hidden from Earth (blue and red), of which 79% are NOT in permanent Sun shadow (blue). A summary of these numbers is shown in Table 1.

4.3. Illumination study

We then used the Kaguya topography data to conduct a comprehensive illumination study. We chose the year 2020 as it is the current goal for returning to the Moon with people, and indeed the south pole is one of the candidate outpost sites. The main purposes of this study were twofold: (1) to determine illumination profiles of key areas including mapping the times and durations of eclipse and (2) to investigate seasonal variations in lighting conditions.

First we produced a quantitative illumination map for 2020 by running simulations for every 12 h for the entire year and then combining the results to show the percentage of time that a point on the surface saw the Sun. This is shown in Fig. 4.

5. Illumination profiles

From the 2020 annual average illumination map we identified several sites that receive the most illumination. These were a point on the rim of Shackleton crater (Point A, 89.68°S, 166.0°W), a point on a ridge close to Shackleton crater (Point B, 89.44°S, 141.8°W), a point on the rim of De Gerlache crater (Point C, 88.71°S, 68.7°W), a point on a small ridge emanating along the 120°E longitude line from the rim of Shackleton crater (Point D, 99.79°S, 124.5°E), and

Table 1
Shows the area within 4° latitude of the south pole that is permanently Sun shadowed, Earth shadowed, and shadowed from both. The colors refer to the areas shown in Fig. 3.

Terrain	Area (km^2)	Fig. 3, color
Sun shadowed	5058	Yellow or red
Sun and Earth shadowed	2653	Red
Earth shadowed	10,520	Blue or red

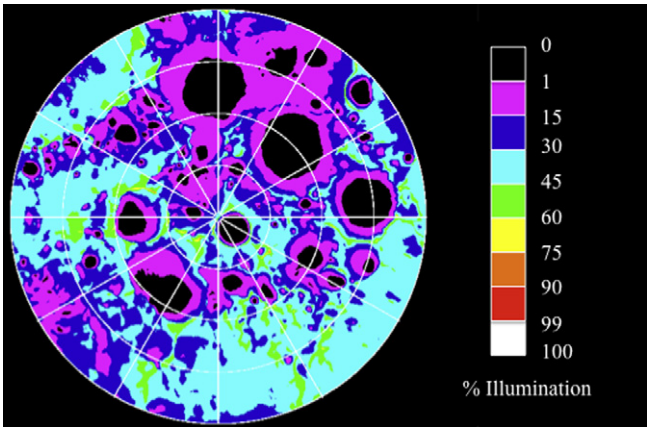

Fig. 4. A quantitative illumination map showing the percentage of time that a point on the surface is illuminated during the year 2020. The map covers from 86°S to the pole, 0° longitude is towards the top of the image.

two points on Malapert Mountain. Points A–D are all illuminated for greater than 80% of the year, and correspond to locations that were identified in the Clementine study as receiving the most illumination in winter (Bussey et al., 1999). The two areas on Malapert are illuminated for greater than 70% of the entire year. The locations of these sites are shown in Fig. 5.

For each of these areas of interest we plotted out the detailed 2020-illumination history. Due to solar symmetry we only need to plot out 6 months worth of data, from mid-summer to mid-winter, in order to still characterize the year's lighting conditions. These are shown in Figs. 6a–d. In all of these plots we show whether a location is lit or dark for a variety of illumination conditions. These polar plots show sub-solar longitude as the angle and sub-solar latitude as the radius. Summer therefore corresponds to the data points in the center of the spiral, corresponding to the most negative sub-solar latitudes. Each sub-solar longitude has six data points corresponding to half a lunar year.

Point D is the most illuminated point that we found with an annual mean illumination of 86%. It is lit for longer than 5 continuous months centered on mid-summer (Fig. 6a). The total duration of eclipse during a 7 month period is one eclipse of approximately 2 days, when the Sun is coming from the 285°W direction. The longest eclipse period in 2020 lasts for approximately 11.5 days during mid-winter.

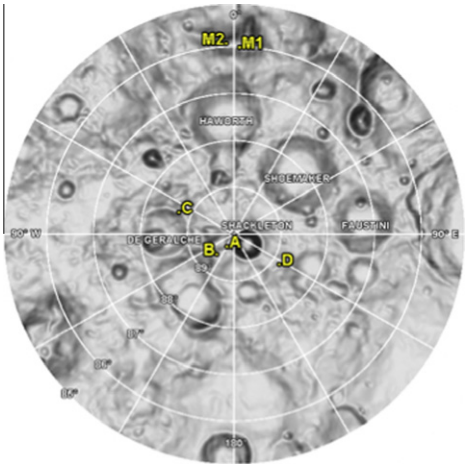

Fig. 5. Map showing the areas identified in this study that received the most illumination. The background image is an "airbrush-effect" image made using the Kaguya topography to show the regional context. The map covers from 85°S to the pole, 0° longitude is towards the top of the image.

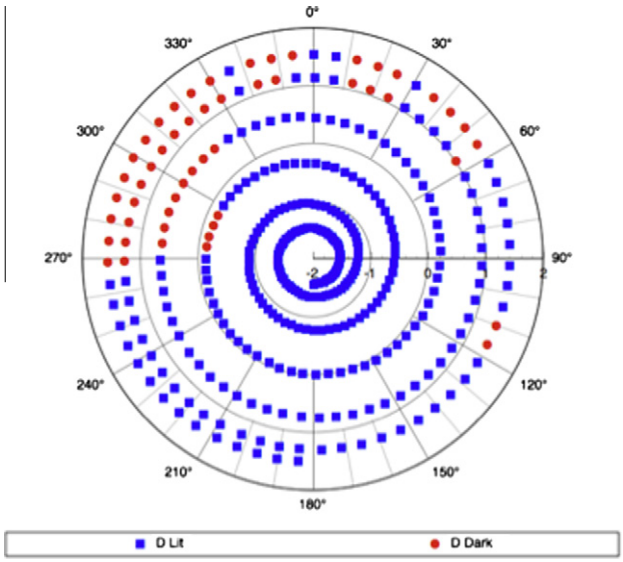

Fig. 6a. Detailed illumination profile for Point D. This area is continuously lit for longer than 5 months during the summer.

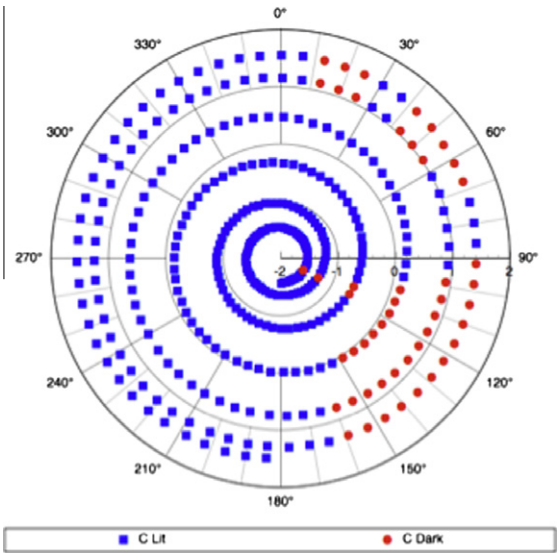

Fig. 6c. Detailed illumination profile for Point C on the rim of De Gerlache crater. Point C has the shortest maximum single eclipse period of any area we looked at, of ~6 days.

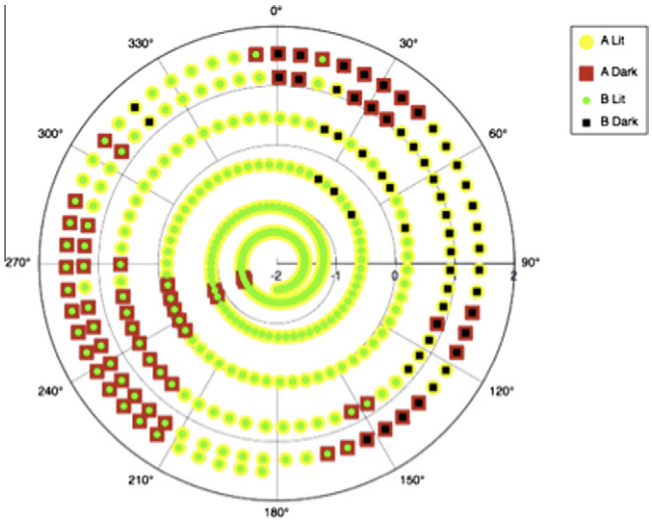

Fig. 6b. A detailed illumination profile for Points A and B. Point B is lit for longer than 4.5 months in the summer and only experiences a total of 4.5 days of eclipse over an 8-month period. Collectively Points A and B appear to be lit 94% of the time.

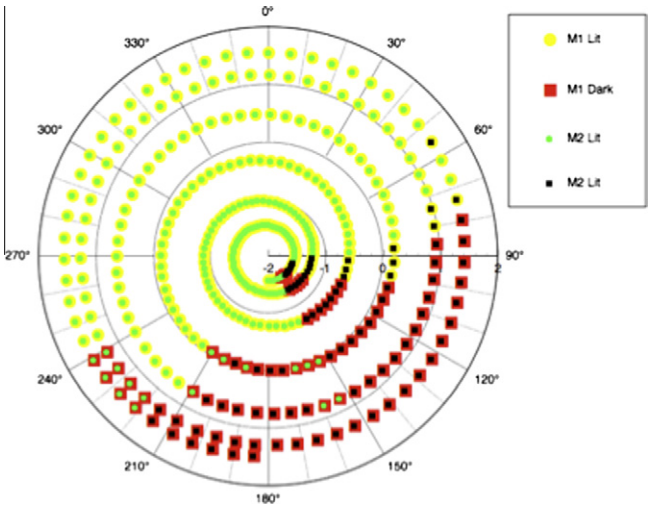

Fig. 6d. Detailed illumination profiles for areas M1 and M2 on Malapert Mountain.

Point B has an annual mean illumination of 82% and also receives constant illumination for more than 4.5 continuous months. It experiences only short eclipses (12–24 h) during the 8-month period centered on mid-summer. The total eclipse duration during that 8-month period is 4.5 days. In addition Point B is complimentary with Point A in that when one site is dark, the other is often illuminated. In fact collectively Points A and B are illuminated for over 8 continuous months and greater than ~94% of the time overall (Fig. 6b). Point C has the shortest maximum eclipse period of any area we looked at, of ~6 days (Fig. 6c).

We have also looked at the most illuminated areas on Malapert Mountain. Malapert has long been of interest as a possible lander/outpost site due to the possibility that the peak of Malapert may have continuous line of sight with the Earth (Lowman et al., 2008). The detailed illumination profiles for points M1 (86.04°S, 2.7°E) and M2 (86.00°S, 2.9°W) are shown in Fig. 6d. Total illumination (74%) is less than for other regions that are closer to the pole.

Fig. 7 shows a snapshot of an image over the south pole. It was taken by the Kaguya HD TV camera as the spacecraft approached the south pole from the farside. As well as being a beautiful image, it reveals some information about the regions we have identified that receive the most illumination near the south pole. All the points identified in this study that receive the greatest amounts of illumination can be seen to represent local topographic maximums at each location.

6. Seasonal variations

Due to the symmetrical nature of sub-solar latitude (the Sun is at each sub-solar latitude twice a year) it is only necessary to consider seven lunar days (out of 12) to characterize the annual lighting variations. We chose times so that mid-summer in 2020 for the southern hemisphere occurred at "noon" on lunar-day one, heading to mid-winter for the seventh lunar day. We produced a quantitative illumination map for each lunar day, showing the

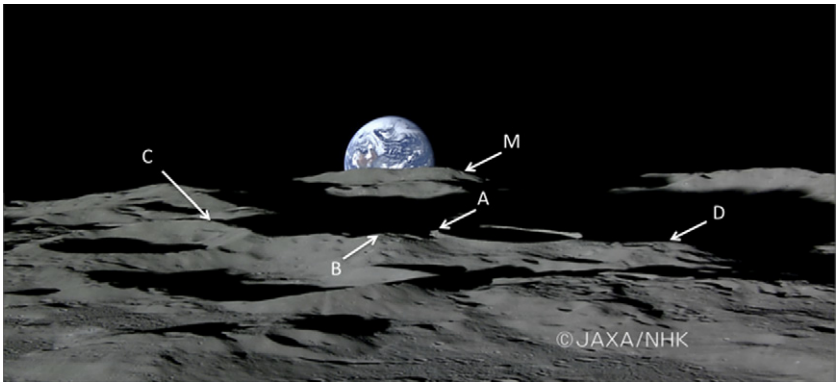

Fig. 7. HD TV image from Kaguya that shows all the areas of interest we identified in this paper. Image courtesy of JAXA. Malapert Mountain is labeled "M".

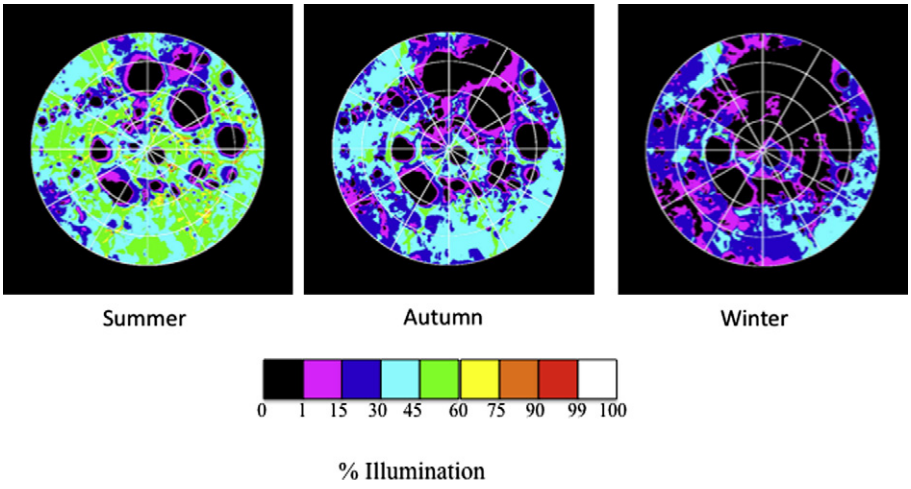

Fig. 8. Quantitative illumination maps for lunar days in summer, autumn, and winter. Each map covers from 86°S to the pole. The 0° longitude line is towards the top of each image.

Table 2
Seasonal variations in lighting conditions for the points of interest identified in this study. Day 1 represents mid-summer for the Moon's summer hemisphere with mid-winter occurring during Day 7. The number shows what percentage of the time a point was illuminated for any particular day. "100" therefore represents that a location was lit for the entire day.

	Point A (89.68°S 166.0°W)	Point B (89.44°S 141.8°W)	Point C (88.71°S 68.7°W)	Point D (88.79°S 124.5°E)	Point M1 (86.04°S 2.7°E)	Point M2 (86.00°S 2.9°W)
Day 1	98	100	98	100	95	90
Day 2	97	100	98	100	92	83
Day 3	97	95	97	100	88	83
Day 4	92	90	86	93	69	75
Day 5	73	64	71	80	64	66
Day 6	51	56	66	63	54	58
Day 7	44	56	64	58	54	58
2020 Mean	81	82	85	86	74	74

percentage of time that a point on the surface received illumination. Fig. 8 shows the quantitative illumination maps for summer, autumn, and winter. Table 2 shows that percentage of time that each point in this study is illuminated for each of the seven lunar days that characterize the lunar illumination year.

7. Conclusions

We have used the Kaguya laser altimeter-derived topography to conduct a comprehensive study of the illumination conditions at and near the Moon's south pole. We have determined, by comparing simulated and actual Clementine images, that the Kaguya topography can be used to generate realistic illumination conditions. We generated an average illumination map for the year 2020 for the lunar south pole region. From this we identified the areas that receive the most illumination. The place receiving the most illumination (86% of the year) is located close to the rim of Shackleton crater at 88.74°S 124.5°E. However two other areas, less than 10 km apart from each other, are collectively lit for 94% of the year. We found that sites exist near the south pole that are

continuously lit for several months during summer. We were also able to map the locations and durations of eclipse periods for these areas. Finally we analyzed the seasonal variations in lighting conditions, from summer to winter, for key areas near the south pole. We conclude that areas exist near the south pole that have illumination conditions that make them ideal candidates as future outpost sites.

Recently released international lunar data is helping us to better understand these interesting locations for future exploration (Spudis et al., 2008). Future topography data (e.g. full-resolution Kaguya and LRO data) will help us to further refine our understanding of the lighting conditions in the polar regions.

Acknowledgments

We thank JAXA for releasing the topography data. This work was funded by the NASA Lunar Science Institute.

References

Bussey, D.B.J., Spudis, P.D., Robinson, M.S., 1999. Illumination conditions at the lunar south pole. Geophys. Res. Lett. 26, 1187–1190.

Bussey, D.B.J., Robinson, M.S., Edwards, K., Cook, A.C., Watters, T., 2001. Simulation of illumination conditions at the lunar south pole. Lunar Planet. Sci. Abstract #1907.

Bussey, D.B.J., Lucey, P.G., Robinson, M.S., Spudis, P.D., Edwards, K.D., Steutel, D., 2003. Permanent shadow in simple craters near the lunar poles. Geophys. Res. Lett. 30 (6).

Bussey, D.B.J., Fristad, K.E., Schenk, P.M., Robinson, M.S., Spudis, P.D., 2005. Constant illumination at the lunar north pole. Nature 434, 842.

Kato, M., Sasaki, S., Tanaka, K., Iijima, Y., Takizawa, Y., 2008. The Japanese lunar mission SELENE: Science goals and present status. Adv. Space Res. 42, 294–300.

Lowman, P.D., Sharpe, B.L., Schrunk, D.G., 2008. Moonbase Malapert? Making the case. Aerosp. Am. (October), 38–43.

Margot, J.L., Campbell, D.B., Jurgens, R.F., Slade, M.A., 1999. Topography of the lunar poles from radar interferometry: A survey of cold trap locations. Science 284, 1658–1660.

Noda, H., Araki, H., Goossens, S., Ishihara, Y., Matsumoto, K., Tazawa, S., Kawano, N., Sasaki, S., 2008. Illumination conditions at the lunar polar regions by KAGUYA (SELENE) laser altimeter. Geophys. Res. Lett. 35. L24203.

Nozette, S., and 33 colleagues, 1994. The Clementine mission to the Moon: Scientific overview. Science 266, 1835–1839.

Nozette, S., Spudis, P.D., Robinson, M., Bussey, D.B.J., Lichtenberg, C., Bonner, R., 2001. Integration of lunar polar remote-sensing data sets: Evidence for ice at the lunar south pole. J. Geophys. Res. 106 (E19), 23253–23266.

Paige, D.A., and 25 colleagues, 2010. Diviner Lunar Radiometer Experiment: Early Mapping Mission Results.

Pike, R.J., 1977. Size-dependence in the Shape of Fresh Impact Craters on the Moon. Impact and Explosion Cratering. Pergamon Press. pp. 489–509.

Spudis, P.D., Bussey, B., Plescia, J., Josset, J., Beauvivre, S., 2008. Geology of Shackleton crater and the south pole of the Moon. Geophys. Res. Lett. 35. L14201. doi:10.1029/2008GL034468.

Vasavada, A.R., Paige, D.A., Wood, S.E., 1999. Near-surface temperatures on Mercury and the Moon and the stability of polar ice deposits. Icarus 141, 179–193.

Ward, W.R., 1975. Past orientation of the lunar spin axis. Science 189, 377–379.

Zuber, M.T., Garrick-Bethell, I., 2005. What do we need to know to land on the Moon again? Science 310, 983–985.